

See discussions, stats, and author profiles for this publication at: <https://www.researchgate.net/publication/236190381>

# High-Efficiency Single-Chirality Separation of Carbon Nanotubes Using Temperature-Controlled Gel Chromatography

ARTICLE *in* NANO LETTERS · APRIL 2013

Impact Factor: 13.59 · DOI: 10.1021/nl400128m · Source: PubMed

---

CITATIONS

39

---

READS

40

4 AUTHORS, INCLUDING:



[Huaping Liu](#)

Chinese Academy of Sciences

44 PUBLICATIONS 727 CITATIONS

SEE PROFILE

# High-Efficiency Single-Chirality Separation of Carbon Nanotubes Using Temperature-Controlled Gel Chromatography

Huaping Liu,<sup>†,‡</sup> Takeshi Tanaka,<sup>†</sup> Yasuko Urabe,<sup>†,‡</sup> and Hiromichi Kataura<sup>\*,†,‡</sup>

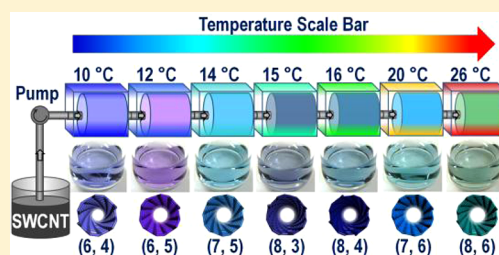
<sup>†</sup>Nanosystem Research Institute, National Institute of Advanced Industrial Science and Technology (AIST), Tsukuba, Ibaraki 305-8562, Japan

<sup>‡</sup>Japan Science and Technology Agency, CREST, Kawaguchi, Saitama 330-0012, Japan

**S** Supporting Information

**ABSTRACT:** We report the use of temperature-controlled gel chromatography for the high-efficiency single-chirality separation of single-wall carbon nanotubes (SWCNTs). This new method uses temperature to selectively control the interaction between the sodium dodecyl sulfate (SDS)-wrapped SWCNTs and an allyl dextran-based gel. Temperature control enhances the differences in the interactions of various  $(n, m)$  SWCNTs with the gel, enabling the separation of high-purity  $(n, m)$  single-species in a single-step process. With this technique, we successfully sorted seven  $(n, m)$  single-species including (6, 4), (6, 5), (7, 5), (8, 3), (8, 4), (7, 6), and (8, 6) from raw HiPco-SWCNTs at a series of temperatures. Our technique offers the advantages of technical simplicity, low cost, and high yield, representing an important step toward the industrial-scale separation of single-chirality SWCNTs.

**KEYWORDS:** Carbon nanotubes, single-chirality separation, gel chromatography, temperature control, high efficiency, industrial scale



Producing populations of single-wall carbon nanotubes (SWCNTs) with single chirality and identical properties is critical for applications in electronics, optoelectronics, and biomedicine.<sup>1–4</sup> Several techniques have been reported for sorting SWCNT mixtures individually dispersed in aqueous solution.<sup>5–15</sup> Several of these methods achieved the high-purity separation of metallic and semiconducting SWCNTs,<sup>5–12</sup> whereas others realized selective enrichment of certain specific chiralities.<sup>10–16</sup> Density gradient ultracentrifugation<sup>14</sup> and ion exchange chromatography<sup>15,16</sup> can isolate many different  $(n, m)$  single-chirality species. However, these two methods have the disadvantages of high cost and limited scalability, preventing the industrial separation of SWCNTs for commercial applications.

Recently, we developed a multicolumn gel chromatography<sup>17,18</sup> technique to separate 13 different  $(n, m)$  species from a HiPco-SWCNT mixture<sup>19</sup> by exploiting the C–C bond curvature-dependent interaction between sodium dodecyl sulfate (SDS)-wrapped SWCNTs and an allyl dextran-based gel (Sephacryl S-200 HR, GE Healthcare, Little Chalfont, UK). Pouring an excess of a HiPco-SWCNT dispersion into multistage columns sorts the SWCNTs based on chirality across the different gel columns with a gel interaction strength index ranging from strongest to weakest. This novel, simple separation method dramatically decreases the cost and significantly improves the separation efficiency of the single-chirality species because an inexpensive SDS surfactant is used as both the dispersant and the eluent for the SWCNTs and because the gel medium can be reused.<sup>17</sup>

The main challenge in the  $(n, m)$  sorting of the HiPco-SWCNTs via multicolumn gel chromatography is in discriminating multiple species that differ only slightly in bond curvature and have minute differences in their interactions with the gel. To address this issue, we took two critical steps:<sup>17</sup> (i) Loading an excess quantity of the SWCNT dispersion (that is, overloading) to induce the competitive adsorption of various  $(n, m)$  SWCNTs on different gel columns, thus sorting by chirality; and (ii) repeating the sorting process to achieve high-purity single-chirality species. In this work, we expanded gel chromatography and employed temperature control to tune the adsorbability of the SDS-wrapped SWCNTs onto the Sephacryl S-200 gel selectively such that one specific single-chirality species from a SWCNT mixture could be solely adsorbed onto the gel columns, thereby allowing the extraction of this single species with high purity. In this method, neither overloading nor repeated separation is necessary.

The present technique is based on the finding that temperatures below room temperature (e.g., 28 °C) selectively decrease the adsorbability of SDS-wrapped HiPco-SWCNTs onto the Sephacryl S-200 gel. By decreasing the temperature to 10 °C, only (6, 4) SWCNTs were able to adsorb to the gel. Applying a HiPco-SWCNT dispersion onto gel columns led directly to the separation of high-purity (6, 4) SWCNTs. Subsequently, increasing the separation temperature by 1 °C enabled the separation of another six different  $(n, m)$  species,

**Received:** January 11, 2013

**Revised:** April 9, 2013

**Published:** April 10, 2013

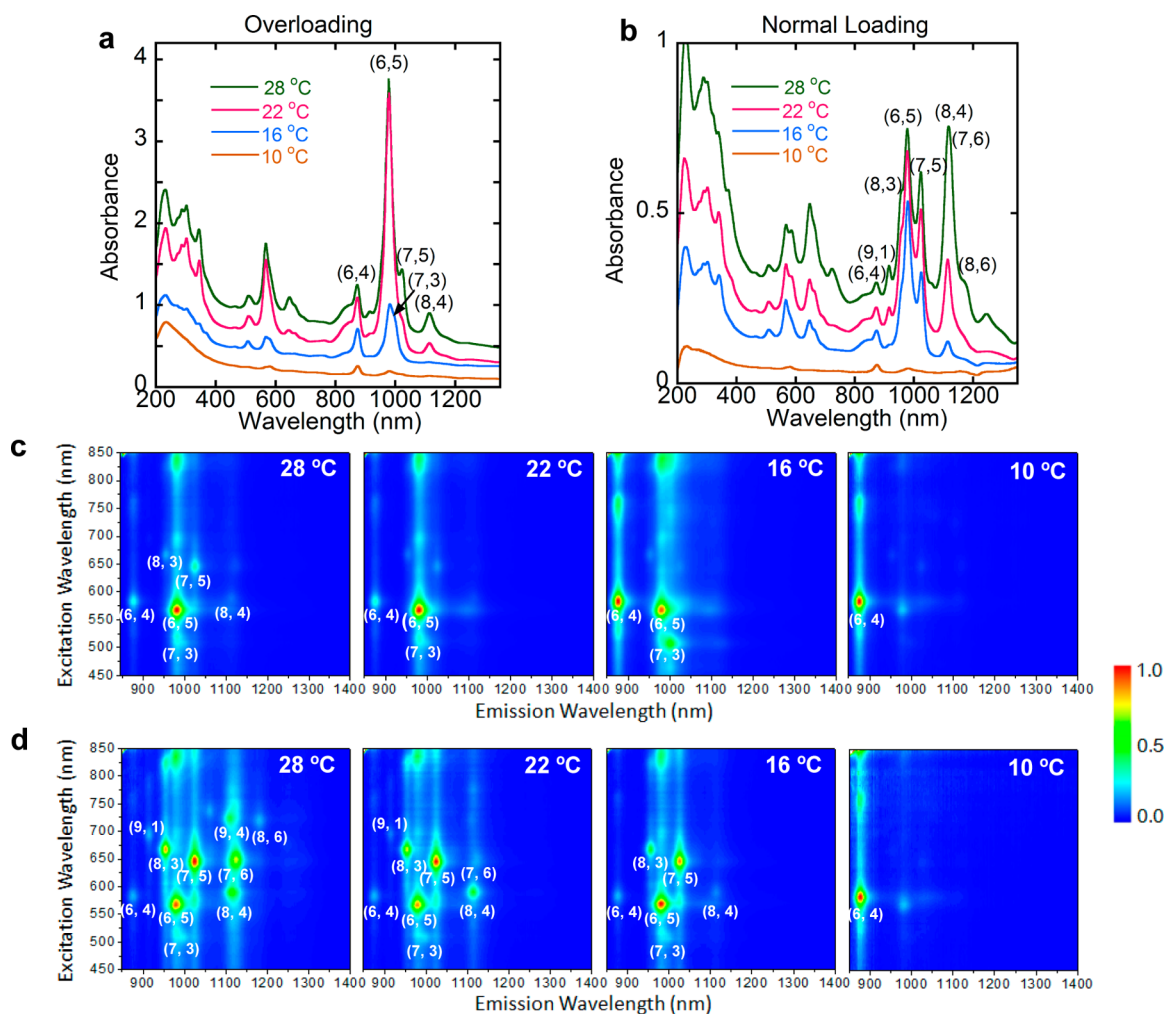


**Figure 1.** Optical characterization of the semiconducting nanotubes adsorbed at different temperatures. (a–b) Optical absorption spectra. (c–d) Photoluminescence contours. (a and c) Overloading (5 mL aliquots of a SWCNT/2 wt % SDS dispersion were loaded onto a column packed with 1.4 mL of gel beads). (b and d) Normal loading (0.5 mL aliquots of a SWCNT/2 wt % SDS dispersion were loaded onto a column packed with 3.5 mL of gel beads). The absorption spectra in a are offset by a constant value to show the changes (10 °C, 0, 16 °C, 0.15, 22 °C, 0.15, 28 °C, 0.30).

(6, 5), (7, 5), (8, 3), (8, 4), (7, 6), and (8, 6), at a series of temperatures by loading the SWCNT fraction at each temperature. With this temperature-controlled gel chromatography method, the high-resolution separation of SWCNTs based on chirality was achieved with dramatically improved separation efficiency. The present technique is the first reported to date in which temperature controls the chirality-selective adsorbability of the SWCNTs. Our analysis indicates that the temperature changes selectively alter the coverage and/or thickness of the SDS coating on the SWCNTs.

The general procedure used for temperature-controlled gel chromatography is as follows: An aqueous dispersion of SWCNTs was prepared by sonicating HiPco-SWCNTs in a 2-wt% SDS aqueous solution (Supporting Information, Figure S1). One column (Tricorn 10/50 column, GE Healthcare) was packed with 1.4 mL of Sephacryl S-200 gel beads (GE Healthcare). To control the separation temperature, the column, SWCNT dispersion, and aqueous SDS eluent solutions were immersed in a water bath (Supporting Information, Figure S2). The effect of the temperature on the adsorbability of the SWCNTs was investigated by overloading the gel column with 5 mL aliquots of the SWCNT dispersion (volume ratio of the SWCNT dispersion and gel beads, 3.6/1) at temperatures

ranging from 30 to 8 °C. The semiconducting SWCNTs adsorbed to the gel column were eluted with a 5 wt % SDS aqueous solution.

The semiconducting SWCNTs that adsorbed at different temperatures were characterized using optical absorption spectra and photoluminescence (PL) contours (Figure 1a, c). The results indicate that overloading induced the adsorption of a (6, 5)-enriched SWCNT mixture that contained five other chiralities, (8, 4), (8, 3), (7, 5), (6, 4), and (7, 3), at 28 °C. With decreasing temperature, the (8, 4), (8, 3), (7, 5), (6, 5), and (7, 3) nanotubes successively lost their adsorbability, and the chirality distribution of the adsorbed SWCNTs became increasingly narrow (Supporting Information, Figure S3). At 10 °C, only (6, 4) SWCNTs were adsorbed. With further temperature decreases, no additional SWCNT adsorption was observed. These results sufficiently demonstrate that lowering the temperature can selectively decrease the adsorbability of SDS-wrapped SWCNTs onto the gel.

To clarify the role of overloading, we further investigated the effect of temperature on the adsorbability of SWCNTs using normal gel chromatography, in which the quantity of the SWCNT dispersion loaded is much smaller than that of the gel; thus, the gel column has adequate space for the adsorption of

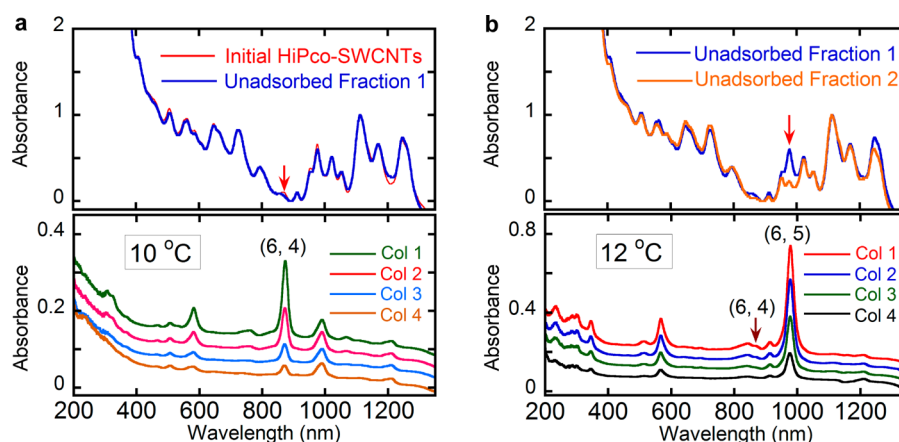


**Figure 2.** Optical absorption analysis of the nanotube fractions separated on multistage gel columns using temperature control. (a) Separation at 10 °C (initial separation temperature). (b) Separation at 12 °C. The upper panels present the corresponding normalized absorption spectra of the loaded and unadsorbed SWCNT fractions. The original spectra are shown in Figure S6 (Supporting Information). The lower panels present the absorption spectra of the separated semiconducting fractions from different columns. These spectra are offset from that for Col. 4 by a constant value to show the changes (in a, Col. 3, 0.03, Col. 2, 0.06, Col. 1, 0.09; in b, Col. 3, 0.05, Col. 2, 0.1, Col. 1, 0.15). The fraction loaded at 12 °C is the fraction not adsorbed at 10 °C (indicated as Unadsorbed Fraction 1). Col = Column.

all adsorbable SWCNTs. In these experiments, 0.5 mL aliquots of the SWCNT dispersion were loaded onto a column (Tricorn 10/50 column) packed with 3.5 mL of Sephacryl S-200 gel beads at varying temperatures (volume ratio of the SWCNT dispersion and gel beads, 1/7). As shown in Figure 1b and d, the absorption spectra and PL contours indicate that, compared with the spectra for the overloading conditions, the spectra for the adsorbed SWCNTs under normal loading conditions were indicative of a much wider chirality distribution at each temperature, except 10 °C, suggesting that all adsorbable nanotubes were adsorbed. Similar to what we observed for overloading, lowering the separation temperature led to a selective decrease in the chirality of the adsorbed SWCNTs under normal loading conditions (Supporting Information, Figure S3). At 10 °C, only the (6, 4) SWCNTs were trapped by the gel, indicating that overloading does not contribute to the adsorption of high-purity (6, 4) SWCNTs.

Because lowering the temperature can selectively decrease the adsorbability of SWCNTs onto the gel and can result in the separation of high-purity (6, 4) SWCNTs at 10 °C, increasing the temperature from 10 °C can conversely enhance the chirality-selective adsorption of the SWCNTs onto the gel. We expected that gradually increasing the separation temperature from 10 °C would allow additional different single high-purity ( $n, m$ ) species to be selectively extracted from the unadsorbed SWCNTs.

To test this hypothesis, we set 10 °C as the starting separation temperature and employed multistage gel columns to improve the separation efficiency (Supporting Information, Figure S4). Several gel columns were connected end-to-end with high-pressure tubes ( $\varnothing$  0.3 mm) in series. A HiPco-SWCNT/2 wt % SDS dispersion was injected into the first column using a peristaltic pump and was allowed to flow through the column series. Figure 2a shows the optical absorption spectra of the adsorbed SWCNT fractions on the gel columns and of the unadsorbed SWCNT fraction. The adsorbed SWCNT fractions were all (6, 4)-enriched SWCNTs (lower panel). Among these fractions, the Column 1 fraction exhibited the strongest (6, 4) absorbance, indicating that it contained the highest (6, 4) concentration. For the other columns, the (6, 4) concentration gradually decreased. Finally,

no SWCNTs could be detected in the eluents from the sixth column (Supporting Information, Figure S5). Compared with the initial SWCNT dispersion, the unadsorbed nanotubes had a lower absorbance for (6, 4) SWCNTs (upper panel in Figure 2a, indication with an arrow), implying that the (6, 4) nanotubes had been selectively separated from the initial SWCNT mixture.

The extraction of the (6, 4) SWCNTs from the SWCNT mixture is a critical step in the separation of other high-purity ( $n, m$ ) SWCNTs at a higher temperature. To separate the next ( $n, m$ ) SWCNTs, we increased the separation temperature to 12 °C and loaded the gel columns with the SWCNT fraction not adsorbed at 10 °C. In Figure 2b, we present the optical absorption spectra for the SWCNT fractions separated on the gel columns together with the loaded SWCNT mixture and the fraction not adsorbed at this stage. The separated fractions were all highly enriched with (6, 5) SWCNTs (lower panel), and no signal for the (6, 4) nanotubes was detected, confirming their complete removal during the previous stage. As observed for the separation of the (6, 4) nanotubes, the Column 1 fraction contained the highest concentration of (6, 5) SWCNTs. In the remaining columns, the (6, 5) SWCNT concentration gradually decreased. A comparison of the loaded and unadsorbed fractions (upper panel in Figure 2b, indication with an arrow) clearly indicates that the (6, 5) SWCNTs were extracted from the loaded SWCNT mixture, given the decrease in their optical absorbance. A slight decrease in the (6, 4) peak is inevitable due to irreversible adsorption, which is a ubiquitous problem in liquid chromatography. These results encouraged us to continue separating additional single-chirality species by increasing the separation temperature.

To separate additional ( $n, m$ ) SWCNTs, the separation temperature was incrementally increased by 1 °C. A chirality separation was performed at each new temperature by loading the unadsorbed SWCNT fraction from the previous stage until no SWCNTs adsorbed to the gel columns. Finally, we successfully separated seven single-chirality species with indices of (6, 4), (6, 5), (7, 5), (8, 3), (8, 4), (7, 6), and (8, 6) at a series of temperatures ranging from 10 to 26 °C (Supporting Information, Figure S7). With further increases in temperature, no additional adsorption of the SWCNTs was observed,



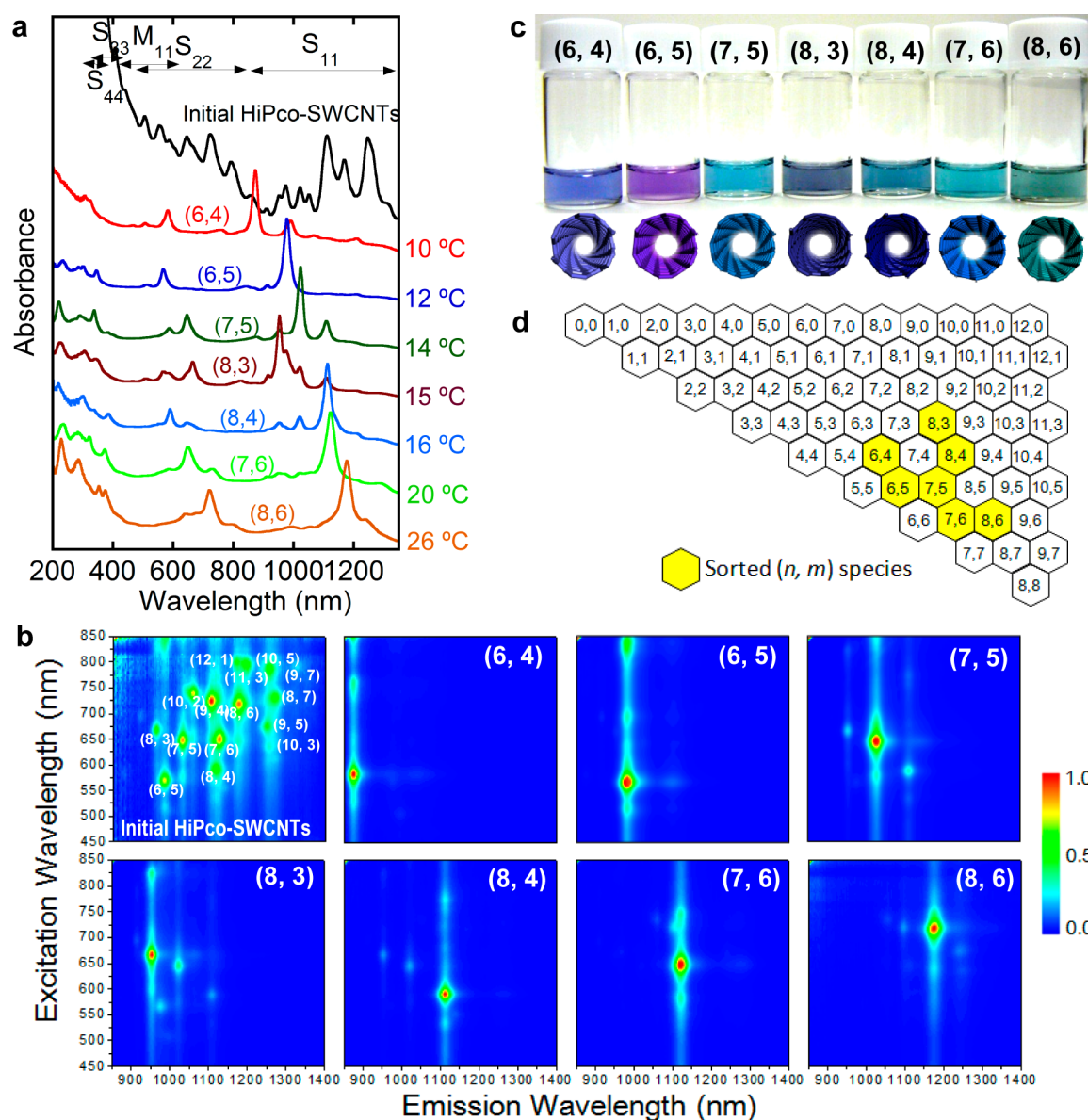


**Figure 3.** Characterization of the purest  $(n, m)$  single-chirality fractions separated at different temperatures (corresponding to Col 1 fractions in Figure 2 and Figure S7 (Supporting Information)). (a) Optical absorption spectra normalized at  $S_{11}$  peaks, shifted vertically for comparison and ranked according to the separation index. (b) Photoluminescence (PL) spectral maps. (c) The solution pictures and corresponding structural models. (d) Location on a chiral map. The optical absorption spectrum and PL map of the initial HiPco-SWCNTs are shown in a and b for comparison.

**Table 1. Evaluation of the Chirality Purity of the Sorted  $(n, m)$  SWCNT Fractions**

$(n, m)$	(6, 4)	(6, 5)	(7, 5)	(8, 3)	(8, 4)	(7, 6)	(8, 6)
separation temperature ( $^{\circ}\text{C}$ )	10	12	14	15	16	20	26
purest fraction <sup>a</sup>	Col 1	Col 1	Col 1	Col 1	Col 1	Col 1	Col 1
purity (%)							
present technique	66	91	58	52	71	73	65
two-step method <sup>17</sup>	46	93	88	56	63	94	89

<sup>a</sup>Col = Column.

suggesting that all adsorbable nanotubes had been separated. In Figure 3a and b, we present the optical absorption spectra and PL maps of the seven separated  $(n, m)$  single species, which are indicated in the chiral map (Figure 3d). Because of their different optical absorption wavelengths, each of the sorted  $(n, m)$  species exhibited a distinct color (Figure 3c). The separation indices for the  $(n, m)$  SWCNTs were identical to

those obtained using the overloading method,<sup>17</sup> in which the separation index is primarily determined by the largest of the three C–C bond curvatures. This result suggests that the effect of temperature on the adsorbability of SWCNTs onto the gel is also strongly dependent on the bond curvature.

The purity of the  $(n, m)$  fractions separated by temperature-controlled gel chromatography was evaluated using the

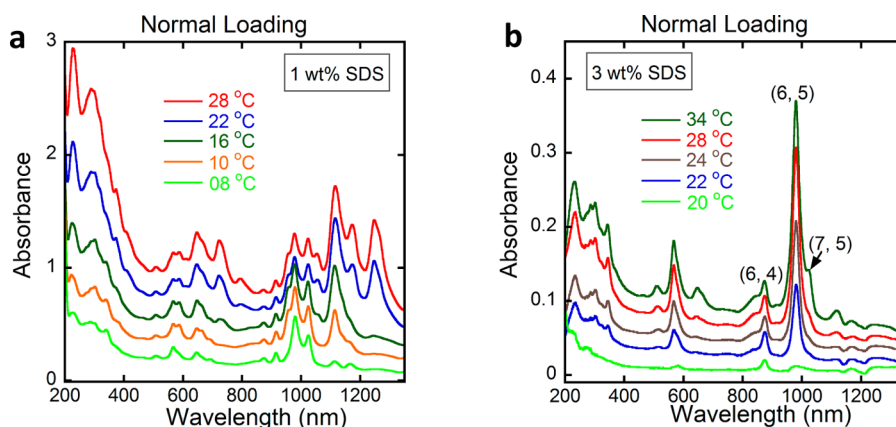


**Figure 4.** Optical absorption spectra of the semiconducting SWCNT fractions adsorbed to a gel column at different temperatures by loading 0.5 mL aliquots of a raw SWCNT/1 wt % SDS dispersion (a) or SWCNT/3 wt % SDS dispersion (b) onto a column packed with 3.5 mL of gel beads. The volume ratio of the loaded SWCNT dispersion to the gel beads was 1/7. The absorption spectra are offset by a constant value to show the changes (in a, 8 °C, 0, 10 °C, 0.1, 16 °C, 0.16, 22 °C, 0.18, 28 °C, 0.12; in b, 20 °C, 0, 22 °C, 0.008, 24 °C, 0.023, 28 °C, 0.026, 34 °C, 0.036).

previously described method.<sup>17</sup> PeakFit software was used to simulate the near-IR optical absorption spectra representing the individual  $(n, m)$  species with wavelengths from 700 to 1350 nm, as shown in Figure S8 (Supporting Information). The purity of each  $(n, m)$  species was computed as the ratio of the area of the dominant absorption peak to the sum of all peak areas; the results are presented in Table 1. Although these  $(n, m)$ -enriched fractions were separated using a single-step process, their purities are comparable to those obtained via the two-step method,<sup>17</sup> with the sorted (6, 4) and (8, 4) SWCNTs exhibiting even higher purities. These results indicate that temperature control significantly increased the differences in the interactions of the  $(n, m)$  SWCNTs with the gel and thus dramatically improved the resolution of the SWCNT chirality separation. More importantly, our present technique is applicable to large gel columns (>200 mL), allowing the high-efficiency and high-yield separation of single-chirality species (Supporting Information, Figure S9). We have provided a video of the separation of the (6, 5) SWCNTs using a 215 mL gel column (Supporting Information, Movie S1). These results led us to propose that a multistage temperature-controlled system could be used for the mass separation of different  $(n, m)$  species in a single step (Supporting Information, Figure S10).

We also investigated the possibility of separating single-chirality species from HiPco-SWCNT mixtures suspended in solutions with different SDS concentrations using temperature-controlled gel chromatography under normal loading conditions (volume ratio of the SWCNT dispersion and gel beads, 1/7). For this experiment, a 0.5 mL aliquot of the raw SWCNT dispersion with 1 wt % SDS or 3 wt % SDS were loaded onto a column packed with 3.5 mL of gel beads at each temperature. The optical absorption spectra of the adsorbed SWCNTs at different temperatures are provided in Figure 4. Our results indicate that, as with the SWCNT/2 wt % SDS dispersion (Figure 1b), reducing the temperature induced a chirality-selective decrease in the adsorbed SWCNTs.

Increasing the SDS concentration in the SWCNT dispersions also selectively decreased the adsorbability of the SWCNTs. For the SWCNT/1 wt % SDS dispersion (Figure 4a), the adsorbed semiconducting SWCNT fraction exhibited a wide chirality distribution. Even at 8 °C, the adsorbed SWCNTs contained a mixture of various semiconducting species. Below 8 °C, the SDS molecules in the 1 wt % SDS solution began to

crystallize, interfering with the gel chromatography process. These results indicate that single-chirality SWCNTs are difficult to separate from SWCNT dispersions with SDS concentrations below 1 wt % but that the enhanced adsorbability of SWCNTs onto the gel enables the separation of additional single-chirality species by diluting the SDS after the extraction of  $(n, m)$  single-chirality SWCNTs from the SWCNT/2 wt % SDS dispersion.

For the SWCNT/3 wt % SDS dispersion, only a (6, 5)-enriched SWCNT mixture with a narrow chirality distribution was adsorbed by the gel column, even at temperatures of up to 34 °C (Figure 4b). With a decrease in the temperature, the adsorbability of the (6, 5) SWCNTs decreased rapidly. At 20 °C, only (6, 4) SWCNTs were adsorbed onto the gel column, indicating that single-chirality separation from SWCNT/3 wt % SDS dispersions can be achieved at temperatures above 20 °C. The temperatures can be easily controlled using a common air conditioner, simplifying the SWCNT separation; however, the number of isolable structures is limited. These results indicate that SWCNT dispersions with varying SDS concentrations exhibit different temperature-dependent adsorption behaviors on Sephacryl gel. The SDS concentration is an important parameter when temperature control is employed to separate SWCNTs.

A higher SDS concentration in the SWCNT dispersion allows the adsorption of additional SDS molecules onto the nanotube surface.<sup>20</sup> The decrease in the adsorbability of the SWCNTs at higher SDS concentrations indicates that the degree of coverage by SDS and/or the thickness of the SDS coating on the nanotube surface determines the adsorbability of the SWCNTs onto the gel. Because decreasing the temperature similarly leads to a weakened adsorbability of the SWCNTs, temperature decreases most likely induce the adsorption of additional SDS molecules onto the SWCNT surfaces and thus the formation of thicker SDS coatings. The effect of temperature on the characteristics of the SDS surfactant in aqueous solutions has been reported.<sup>21,22</sup> Each SDS solution has a Krafft temperature,<sup>21</sup> below which the surfactant molecules tend to aggregate and form a nonsoluble phase. For example, the Krafft temperatures of aqueous SDS solutions with concentrations of 1 wt %, 2 wt %, 3 wt %, and 5 wt % are, respectively, 14.61, 15.48, 16.29, and 17.34 °C.<sup>21</sup> A higher-concentration SDS solutions clearly has a higher Krafft temperature, meaning that SDS molecules aggregate more

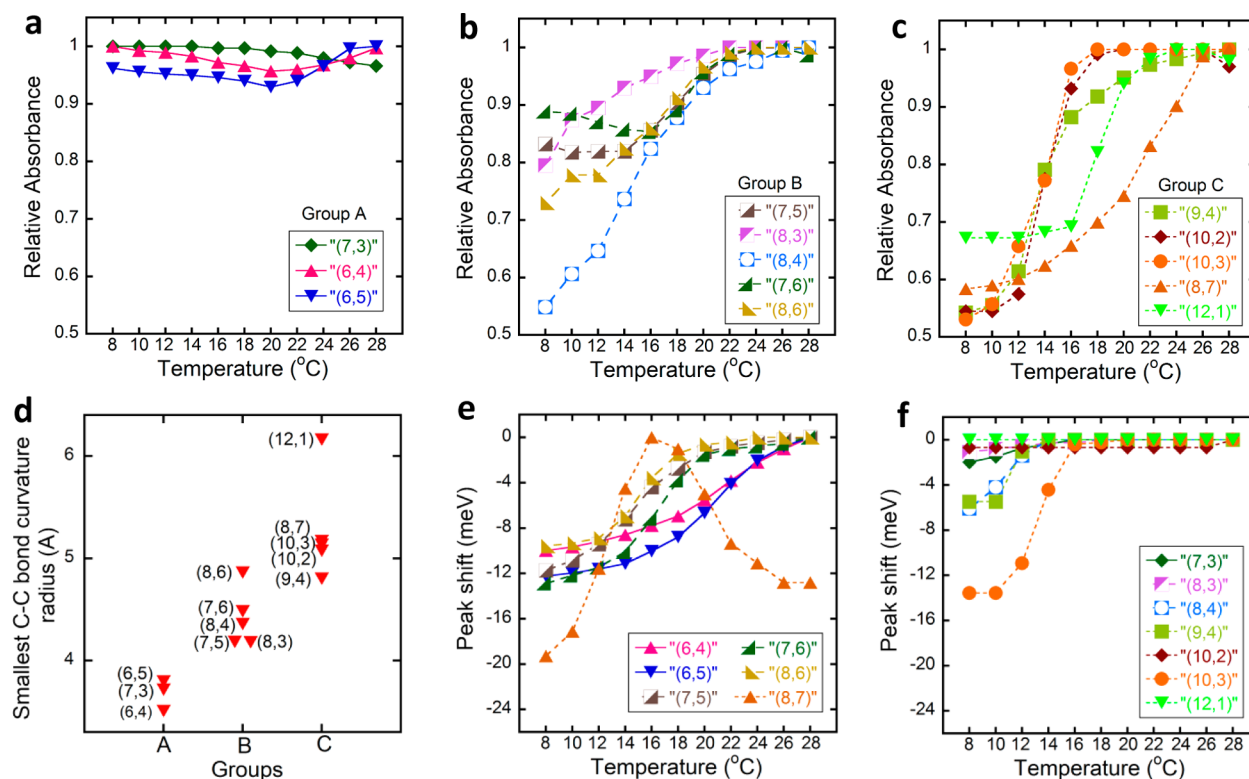


**Figure 5.** (a–c) Plots of the relative optical absorbance of the  $(n, m)$  SWCNT/SDS micelles as a function of temperature. (d) The smallest C–C bond curvature radii of the SWCNTs in (a–c). (e–f) Plots of the spectral shifts for the  $(n, m)$  SWCNT/SDS micelles as a function of temperature.

easily. We speculate that lowering temperature decreases the solubility of the SDS surfactant,<sup>21,22</sup> causing additional SDS molecules to aggregate on the nanotube surfaces, forming high-density SDS coatings, similar to the effect of increasing the SDS concentration. This hypothesis agrees well with the experimental observation that SWCNT/SDS micelles are more difficult to precipitate via centrifugation at lower temperatures (Supporting Information, Figure S11) because SWCNTs with thicker SDS coatings have lower densities.<sup>20,23</sup>

As mentioned above, the separation index of  $(n, m)$  nanotubes is strongly dependent on the largest C–C bond curvature, suggesting that the bond curvature affects the adsorption of SDS molecules and thus the thickness and/or coverage of the SDS coating on the nanotube surface. The largest carbon–carbon bond curvature is closely correlated with the surface curvature of a nanotube.<sup>24</sup> It has been reported that the alkyl tails of SDS surfactants on graphite preferentially align along the crystallographic directions.<sup>25</sup> We can imagine that when a graphene sheet is rolled up into a cylindrical nanotube, the SDS molecules have to bend to form a stable SWCNT/SDS complex. When an SDS molecule wraps a narrower nanotube with a large bond curvature, it encounters a bigger energetic barrier due to bending.<sup>26</sup> The SDS molecules therefore prefer to adsorb to larger-diameter nanotubes with smaller bond curvatures. Lowering the temperature enhances the selective adsorption of SDS molecules based on the SWCNT structures, enlarging the differences in the thickness and/or coverage of the SDS coatings among various nanotubes and resulting in a rapid decrease in the adsorbability of larger-diameter nanotubes with smaller bond curvatures onto the gel. Therefore, reducing the temperature amplifies the already existing differences in the interactions of the various  $(n, m)$  SWCNTs with the gel,

significantly improving the resolution of the SWCNT separation.

The electronic and optical properties of the SWCNTs are sensitive to the surrounding environment.<sup>27–32</sup> To confirm the change in the SWCNTs/SDS complex with temperature, we recorded the optical absorption spectra of 13 types of  $(n, m)$ -enriched SWCNTs suspended in 1 wt % SDS aqueous solution at different temperatures ranging from 8 to 28 °C. We observed spectral quenching and a shift in the center of the absorbance peak with decreasing temperature for each  $(n, m)$  fraction (Supporting Information, Figures S12–13), which are normalized in Figure 5. Based on the magnitude of the temperature effect on the spectral intensities, we divided the 13 different  $(n, m)$  species into three groups (Groups A, B, and C) as shown in Figure 5a, b, and c, respectively. With a decrease in temperature, the spectral intensities of the nanotubes in Group A changed less than 10%, the Group B intensities slowly decreased by 10–30% except for that of (8, 4), and the intensities of Group C (not separated in the present work) sharply decreased by 30–50%. The smallest C–C bond curvature radii of the nanotubes in each group are presented in Figure 5d. The effect of temperature on the absorbance quenching of the SWCNTs clearly increased with an increase in the smallest bond curvature radius. The temperature generally had a greater influence on the spectral shifts of near-armchair SWCNTs (Figure 5e and f), such as (6, 5) and (7, 5), than on the spectral shifts of SWCNTs with smaller chiral angles, such as (8, 3) and (12, 1).

SWCNT bundling has been reported to result in absorbance quenching and peak shifts.<sup>27</sup> To determine the reason for the temperature-dependent absorbance of SWCNT/SDS complexes, the temperature of a SWCNT/1 wt % SDS dispersion was cycled between 20 and 10 °C, and the absorption spectra



were recorded. When the temperature was cycled back to 20 °C from 10 °C, both the absorbance and the peak position were restored (Supporting Information, Figure S14), suggesting that SWCNT bundling is not the primary reason for the absorbance quenching of SWCNT/SDS complexes at reduced temperatures because the as-formed SWCNT bundles can be isolated with difficulty by simply increasing the temperature. Several groups have reported that proton doping could cause the absorbance quenching of SWCNTs.<sup>28,29</sup> To address the effect of temperature on the absorbance spectra of SWCNT/SDS complexes, we added sodium hydroxide to a HiPco-SWCNT/1 wt % SDS dispersion and subsequently recorded the optical absorption spectra at varying temperatures. We found that spectral quenching was suppressed at reduced temperatures, but a clear spectral shift was still observed (Supporting Information, Figure S15). This result demonstrates that spectral quenching at lower temperatures results from proton injection.<sup>28,29</sup> As presented in Figure 5a–d, larger SWCNT bond curvature radii led to easier proton injection. A similar proton injection phenomenon was observed by increasing the SDS concentration in the HiPco-SWCNT dispersion (Supporting Information, Figure S16), indicating that the proton injection was most likely caused by the adsorption of high-density SDS coatings onto the nanotubes. Neutral SWCNTs do not attract ionic species. However, after the adsorption of SDS molecules, the protons [H<sup>+</sup>] in the naturally acidic SWCNT/SDS dispersion (pH ~ 5.0 for 1 wt % SDS; pH ~ 4.4 for 2 wt % SDS; pH ~ 4.1 for 3 wt % SDS) are attracted to the anionic head groups of the surfactants. This behavior agrees well with the absorbance peak broadening of (*n*, *m*) nanotubes observed at reduced temperatures (Supporting Information, Figures S12–13) because the incorporation of the protons [H<sup>+</sup>] into the SDS molecule heads could cause an increase in the intertube interactions due to a reduction in electrostatic repulsion and a decrease in the amount of space between nanotubes.<sup>23,27</sup> At the nanotube sidewalls, the protons react with the preadsorbed oxygen to create hydroperoxide carbocations, creating holes in the SWCNT valence band.<sup>28,29</sup> Therefore, the absorbance quenching could serve as a measure of the differential adsorption of SDS molecules with decreasing temperature based on the SWCNT structures. However, the spectral shift was not clearly observed with increasing SDS concentration in the SWCNT dispersion (Supporting Information, Figure S16). Reducing the temperature may have enhanced the interactions between the adsorbed SDS molecules and nanotubes of certain specific chiralities (e.g., near-armchair SWCNTs) and may have resulted in the reassembly of the SDS molecules on the nanotube surfaces, thus altering the dielectric constant around the SWCNTs and causing a spectral shift.<sup>30–32</sup>

The SDS concentration in SWCNT dispersion greatly affects the temperature-dependent adsorption of SDS molecules onto the nanotube surfaces and thus the adsorbability of SWCNTs on the gel. As shown in Figures 1b and 4a, increasing the SDS concentration from 1 wt % to 2 wt % resulted in a reduction in the adsorbability of the nanotubes in Group C (Figure 5c), even at 28 °C. Thus, the single-chirality separation of these nanotubes was not achieved in the present study, in which the initial SWCNTs were suspended in a 2 wt % SDS aqueous solution. To achieve the separation of the nanotubes in Group C, the SDS concentration has to be reduced from 2 wt % to 1 wt %. Actually, such experimental conditions were used previously to separate 13 different SWCNT chiralities<sup>17</sup>

(although not reported). Further increasing the SDS concentration to 3 wt % eliminated the adsorbability of the nanotubes in Group B (Figures 4b and 5b), leading to that the isolable nanotubes were limited to Group A.

In conclusion, we discovered that the separation temperature could tune the adsorbability of SDS-wrapped SWCNTs onto an allyl dextran-based gel in a chirality-selective manner. Based on this finding, we developed a temperature-controlled gel chromatography technique to significantly improve the resolution of the chirality separation of SWCNTs, thereby allowing the separation of single-chirality SWCNTs in a single-step process. With this technique, seven single-chirality species were separated from HiPco-SWCNTs at a series of temperatures. We believe that additional types of single-chirality SWCNTs can be separated using this technique when used in combination with varying the SDS concentration. This novel technique is superior to all other reported separation methods because of its simplicity, low cost, and high efficiency, and it represents an important step forward in the industrial-scale separation of single-chirality SWCNTs.

## ■ ASSOCIATED CONTENT

### Supporting Information

Details on experimental procedures, supplementary Figures S1–16, and Supplementary Movie S1. This material is available free of charge via the Internet at <http://pubs.acs.org>.

## ■ AUTHOR INFORMATION

### Corresponding Author

\*E-mail: [h-kataura@aist.go.jp](mailto:h-kataura@aist.go.jp). Tel.: +81-29-861-2551. Fax: +81-29-861-2786.

### Notes

The authors declare no competing financial interest.

## ■ REFERENCES

- (1) Avouris, P.; Martel, R. *MRS Bull.* **2010**, *35*, 306–313.
- (2) Yang, L.; Wang, S.; Zeng, Q.; Zhang, Z.; Pei, T.; Li, Y.; Peng, L. P. *Nat. Photon.* **2011**, *5*, 672–676.
- (3) Jain, R. M.; Howden, R.; Tvrđy, K.; Shimizu, S.; Hilmer, A. J.; McNicholas, T. P.; Gleason, K. K.; Strano, M. S. *Adv. Mater.* **2012**, *24*, 4436–4439.
- (4) Robinson, J.; Welsher, K.; Tabakman, S. M.; Sherlock, S. P.; Wang, H.; Luong, R.; Dai, H. *Nano Res.* **2010**, *3*, 779–793.
- (5) Krupke, R.; Hennrich, F.; Löhneysen, H. V.; Kappes, M. M. *Science* **2003**, *301*, 344–347.
- (6) Maeda, Y.; Kimura, S. I.; Kanda, M.; Hirashima, Y.; Hasegawa, T.; Wakahara, T.; Lian, Y.; Nakahodo, Y.; Tsuchiya, T.; Akasaka, T.; Lu, J.; Zhang, X.; Gao, Z.; Yu, Y.; Nagase, S.; Kazaoui, S.; Minami, N.; Shimizu, T.; Tokumoto, H.; Saito, R. *J. Am. Chem. Soc.* **2005**, *127*, 10287–10290.
- (7) Yanagi, K.; Miyata, Y.; Kataura, H. *Appl. Phys. Exp.* **2008**, *1*, 034003.
- (8) Tanaka, T.; Jin, H.; Miyata, Y.; Fujii, S.; Suga, H.; Naitoh, Y.; Minari, T.; Miyadera, T.; Tsukagoshi, K.; Kataura, H. *Nano Lett.* **2009**, *9*, 1497–1500.
- (9) Moshhammer, K.; Hennrich, F.; Kappes, M. M. *Nano Res.* **2009**, *2*, 599–606.
- (10) Tanaka, T.; Liu, H.; Fujii, S.; Kataura, H. *Phys. Status Solidi (RRL)* **2011**, *5*, 301–306.
- (11) Liu, H.; Feng, Y.; Tanaka, T.; Urabe, Y.; Kataura, H. *J. Phys. Chem. C* **2010**, *114*, 9270–9276.
- (12) Arnold, M. S.; Green, A. A.; Hulvat, J. F.; Stupp, S. I.; Hersam, M. C. *Nat. Nanotechnol.* **2006**, *1*, 60–65.
- (13) Tyler, T. P.; Shastry, T. A.; Leever, B. J.; Hersam, M. C. *Adv. Mater.* **2012**, *35*, 4765–4768.



- (14) Ghosh, S.; Bachilo, S. M.; Weisman, R. B. *Nat. Nanotechnol.* **2010**, *5*, 443–450.
- (15) Tu, X.; Manohr, S.; Jagota, A.; Zheng, M. *Nature* **2009**, *460*, 250–253.
- (16) Tu, X.; Walker, A. R. H.; Khripin, C. Y.; Zheng, M. *J. Am. Chem. Soc.* **2011**, *133*, 12998–13001.
- (17) Liu, H.; Nishide, D.; Tanaka, T.; Kataura, H. *Nat. Commun.* **2011**, *2*, 309.
- (18) Liu, H.; Tanaka, T.; Kataura, H. *Phys. Status Solidi B* **2011**, *248*, 2524–2527.
- (19) Nikolaev, P.; Bronikowski, M. J.; Bradley, R. K.; Rohmund, F.; Colbert, D. T.; Smith, K. A.; Smalley, R. E. *Chem. Phys. Lett.* **1999**, *313*, 91–97.
- (20) Duque, J. G.; Densmore, C. G.; Doorn, S. K. *J. Am. Chem. Soc.* **2010**, *132*, 16165–16175.
- (21) Vautier-Giongo, C.; Bales, B. L. *J. Phys. Chem. B* **2003**, *107*, 5398–5403.
- (22) Benrraou, M.; Bales, B. L.; Zana, R. *J. Phys. Chem. B* **2003**, *107*, 13432–13440.
- (23) Niyogi, S.; Densmore, C. G.; Doorn, S. K. *J. Am. Chem. Soc.* **2009**, *131*, 1144–1153.
- (24) Li, J. Q.; Jia, G. X.; Zhang, Y. F.; Chen, Y. *Chem. Mater.* **2006**, *18*, 3579–3584.
- (25) Sammalakorpi, M.; Panagiotopoulos, A. Z.; Haataja, M. *J. Phys. Chem. B* **2008**, *112*, 2915–2921.
- (26) Tummala, N. R.; Striolo, A. *ACS Nano* **2009**, *3*, 595–602.
- (27) Crochet, J. J.; Sau, J. D.; Duque, J. G.; Doorn, S. K.; Cohen, M. *ACS Nano* **2011**, *4*, 2611–2618.
- (28) Dukovic, G.; White, B. E.; Zhou, Z.; Wang, F.; Jockush, S.; Steigerwald, M. L.; Heinz, T. F.; Friesner, R. A.; Turro, N. J.; Brus, L. E. *J. Am. Chem. Soc.* **2004**, *126*, 15269–15276.
- (29) Strano, M. S.; Huffman, C. B.; Moore, V. C.; O'Connell, M. J.; Haroz, E. H.; Hubbard, J.; Miller, M.; Rialon, K.; Kittrell, C.; Ramesh, S.; Hauge, R. H.; Smalley, R. E. *J. Phys. Chem. B* **2003**, *107*, 6979–6985.
- (30) O'Connell, M. J.; Sivaram, S.; Doorn, S. K. *Phys. Rev. B* **2004**, *69*, 235415.
- (31) Nugraha, A. R. T.; Saito, R.; Sato, K.; Araujo, P. T.; Jorio, A.; Dresselhaus, M. S. *Appl. Phys. Lett.* **2010**, *97*, 091905.
- (32) Chiashi, S.; Watanabe, S.; Hanashima, T.; Homma, Y. *Nano Lett.* **2008**, *8*, 3097–3101.